Effect of Angular Velocity of Inner Cylinder on Laminar Flow through Eccentric Annular Cross Section Pipe

Ressan Faris Hamd*
Department of Mechanical Engineering, Kufa University, Iraq
Corresponding author; E-mail address: *Ressan@yahoo.com*

***Abstract*-- This is study investigated the effect increasing the angular velocity on the axial velocity profile and pressure gradient for steady state, three dimensional, incompressible, isothermal, and laminar flow of a Newtonian fluid through eccentric annular duct.**

The results are presented for angular velocity range (0, 50, 100, 150, 200, and 250) rpm at axial Reynolds number 200 based on bulk axial velocity with radius ratio 0.5 where FLUENT software version (6.2) is used to solve continuity and momentum equations. The results of axial and tangential velocity for four sectors were found to be in good agreement with other previously published research at eccentricity are 0.2 and 0.5.

The results show that the axial velocity varies with varying in rotational speed of inner cylinder and the axial pressure gradient increases with increasing in rotational speed. Also when inner cylinder is rotated, the axial velocity profile become non-axisymmetry around center of radial gap of annular pipe at eccentricity of 0.2 and 0.4.

***Index Term*-- annular, rotate cylinder, laminar, eccentric**

NOMENCLATURE

Latin symbols	Description
e	displacement of inner cylinder axis from outer cylinder axis (m)
r	radial distance from axis of inner cylinder (m)
p'	Axial pressure gradient (Pa/m)
R_I	outer radius of inner cylinder (m)
R_O	inner radius of outer cylinder (m)
Re	axial Reynolds number $2\rho U\delta/\mu$ (--)
u	non-dimensional axial component of velocity (--)
v	non-dimensional tangential component of velocity (--)
$\bar{u}$	axial component of velocity (m/s)
$\bar{v}$	tangential component of velocity (m/s)
U	bulk axial velocity (m/s)
w	non-dimensional radial component of velocity (m/s)
x	Cartesian coordinate in horizontal direction (m)
y	Non-dimensional value of distance from outer wall (m)

Greek symbols	Description
ξ	Non-dimensional distance from wall of inner cylinder (--)
κ	Radius ratio R_I/R_O (--)
ε	Eccentricity e/δ (--)
ρ	density of the air (kg/m^3)
ϕ	Azimuthal location with respect to inner cylinder (degree)
δ	Annular gap width $R_O - R_I$ (m)
ω	angular velocity of inner cylinder (rpm)
μ	dynamic viscosity of the fluid (kg/m.s)
ν	kinematic viscosity of the fluid (m^2/s)
symbols	Abbreviations
CFD	Computational Fluid Dynamic

I. INTRODUCTION

The classical Couette flow problem consists of infinitely long concentric cylinders and an incompressible Newtonian fluid between them. For a system with a rotating inner cylinder and a stationary outer cylinder, the fluid flow will pass on stable circular Couette flow and steady axisymmetric Taylor vortex flow for the value of Taylor number *Ta* (or Reynolds number Re) less than and greater than a critical value Ta_c (or Re_c) respectively **[1]**.

The flow device of Taylor–Couette flow comprising concentric rotating cylinders is widely used in many industrial and research processes found in chemical, mechanical and nuclear engineering. The device can be only one cylinder rotating and the other at rest, or two cylinders rotating in the same or counter directions. The accurate calculation of the flow property is important even from the standpoint of the normal operation of the device. The distribution of energy loss in the device may greatly influence the industrial process of mixing, diffusion, heat transfer, and flow stabilities, etc. **[2]**.

C. H. Ataide et al [3]: (2003) analyzed the fluid flow in annular regions is an area of great interest in the petroleum industry, both in the drilling and in the artificial rising of the petroleum. Through the numerical simulation, using the computer fluid dynamics commercial code (CFD). They investigated flow of non-Newtonian fluids flow through the annular space formed by two tubes in concentric and eccentric

arrangements of a horizontal system. They studied contemplates the prediction of effects of viscosity, eccentricity, flow and inner axis rotation velocity over the tangential and axial velocity profiles and over the hydrodynamic losses, considering that these two variables are relevant in the understanding of the drilling fluids flow. They evaluated the performance by using numerical technique, and compared the obtained results with other reported works.

C. Shu et al [1]: (2004) used the differential quadrature (DQ) method to simulate the eccentric Couette–Taylor vortex flow in an annulus between two eccentric cylinders with rotating inner cylinder and stationary outer cylinder. Their approach combining the SIMPLE (semi-implicit method for pressure linked equations). They proposed to solve the time-dependent, three-dimensional incompressible Navier–Stokes equations in the primitive variable form. They obtained eccentric steady Couette–Taylor flow patterns from the solution of three-dimensional Navier–Stokes equations. For steady eccentric Taylor vortex flow, detailed flow patterns were obtained and analyzed. The effect of eccentricity on the eccentric Taylor vortex flow pattern was also studied.

Escudier et al [4]: (2000) showed that there is excellent agreement between their calculations for a Newtonian fluid and experimental data for annuli with 20%, 50%, and 80% eccentricity. Their results are reported for calculations of the flow field, wall shear stress distribution and friction factor for a range of values of eccentricity, radius ratio, and Taylor number. They showed the axial component of velocity is directly affected by the radial/tangential velocity field and rotation of the inner cylinder is found to have a strong influence on the axial velocity distribution. As the Taylor number is increased the friction factor for high values of $\varepsilon > 0.9$ increases.

Escudier et al. [5]: (2002) evaluated the effect of internal cylinder rotation on the laminar flow of non-Newtonian fluids in an eccentric annular region, compared their numerical simulations of two-dimensional flow against experimental data. Their comparison of simulated velocity profiles and those obtained experimentally showed a good agreement. These authors also analyzed the effect of the attrition factor under the influence of the flow condition and the eccentricity of the arrangement.

M. Carrasco Teja et al [6]: (2009) analyzed the effects of rotation and axial motion of the inner cylinder of an eccentric annular duct during the displacement flow between two Newtonian fluids of differing density and viscosity. The annulus is assumed narrow and oriented near the horizontal. The main application is the primary cementing of horizontal oil and gas wells, in which casing rotation and reciprocation is becoming common. In this application it is usual for the displacing fluid to have a larger viscosity than the displaced fluid. They show that steady traveling wave displacements may occur, as for the situation with stationary walls. For small buoyancy numbers and when the annulus is near to concentric, the interface is nearly flat and a perturbation solution can be found analytically. This solution shows that rotation reduces the extension of the interface in the axial direction and also results in an azimuthal phase shift of the steady shape away from a symmetrical profile. They said that the phase shift results in the positioning of heavy fluid over light fluid along segments of the interface. When the axial extension of the interface is sufficiently large, this leads to a local buoyancy-driven fingering instability, for which a simple predictive theory is advanced. Over longer times, the local fingering is replaced by steady propagation of a diffuse interfacial region that spreads slowly due to dispersion. Slow axial motion of the annulus walls on its own is apparently less interesting. There is no breaking of the symmetry of the interface and hence no instability.

Nouri et al [7]: (1993) who experimentally evaluated the annular flow of Newtonian and non-Newtonian fluids in situations above the laminar flow, using the laser anemometry technique to quantify the axial, radial and tangential velocity profiles. Their experimental determinations, however, did not predict the effect of internal axis rotation.

Md Mamunur Rashid [8]: (2008) studied a detailed computational investigation on the Newtonian fluid flow through concentric annuli with centre body rotation with glucose as the working fluid will be carried out. He confined flow through concentric annuli with centre body rotation is examined numerically by solving the modified Navier-Stokes equations. He measured the axial and tangential components of velocity is presented in non-dimensional form for a Newtonian fluid. The annular geometry consists of a rotating Centre body with angular speed of 126 rpm and a radius ratio of 0.506. He integrated continuity and the momentum equations numerically with the aid of a finite – volume method. Your numerical predictions have been confirmed by comparing them with experimentally derived axial and tangential velocity profiles obtained for a Newtonian. For the Newtonian (Glucose) fluid, he was carried out for Reynold's number of 800 and 1200.

II. Governing Equations and Boundary Conditions

Consider steady state, isothermal, laminar, and fully developed flow of fluids for which the density and the viscosity are constant. The governing partial differential equation in cylindrical coordinate for this case become [12]

Continuity equation:

$$\frac{\partial}{\partial r}(wr)+\frac{\partial v}{\partial \phi}=0 \quad (1)$$

u-Momentum equation:

$$\rho\left(w\frac{\partial u}{\partial r}+\frac{v}{r}\frac{\partial u}{\partial \phi}\right)=-\frac{\partial p}{\partial z}+\frac{\mu}{r}\frac{\partial}{\partial r}\left(r\frac{\partial u}{\partial r}\right)+\frac{\mu}{r^2}\frac{\partial^2 u}{\partial \phi^2} \quad (2)$$

v-Momentum:

$$\rho\left(w\frac{\partial v}{\partial r}+\frac{v}{r}\frac{\partial v}{\partial \phi}+\frac{wv}{r}\right)=-\frac{1}{r}\frac{\partial p}{\partial \phi}+\frac{\mu}{r^2}\frac{\partial}{\partial r}\left[r^3\frac{\partial}{\partial r}\left(\frac{v}{r}\right)+r\frac{\partial w}{\partial \phi}\right]$$
$$+\frac{2\mu}{r}\frac{\partial}{\partial \phi}\left(\frac{1}{r}\frac{\partial v}{\partial \phi}+\frac{w}{r}\right) \quad (3)$$

w-Momentum:

$$\rho\left(w\frac{\partial w}{\partial r}+\frac{v}{r}\frac{\partial w}{\partial \phi}-\frac{v^2}{r}\right)=-\frac{\partial p}{\partial r}+\frac{2\mu}{r}\frac{\partial}{\partial r}\left(r\frac{\partial w}{\partial r}\right)$$
$$+\frac{\partial}{\partial \phi}\left[\mu\frac{\partial}{\partial r}\left(\frac{v}{r}\right)\right]+\frac{\mu}{r^2}\frac{\partial^2 w}{\partial \phi^2} \quad (4)$$

with boundary conditions:

$u = v = w = 0$ on the outer cylinder;

$u = w = 0$ and $v = \omega.R_I$ on the inner cylinder;

$\dot{m} = c$ at inlet (axial flow in z-direction)

other terms define as:

$$\delta = R_O - R_I$$

$$\kappa = \frac{R_I}{R_O}$$

$$\varepsilon = \frac{e}{R_O - R_I}$$

$$\mathrm{v} = \frac{\bar{\mathrm{v}}}{R_i\omega}$$

$$u = \frac{\bar{u}}{U}$$

$$\zeta = \frac{r - R_i}{R_o - R_i}$$

$$\mathrm{Re} = \frac{2\rho U\delta}{\mu}$$

$$Ta = \left(\frac{\rho\omega}{\mu}\right)^2 R_I\delta^3$$

III. Grid Generation

Total grid for the problem is generated by using commercial grid generator GAMBIT (2.2.30) in three dimension of annular passage at eccentricity of 0.2 & 0.4. Grid structure is created here and it consists of non-uniform hexahedral wedge element having 91,200 cells and 102,960 nodes. The grid was employed of the problem consists of 240 radial, 10 circumferential and 40 axial grid-lines as shown in Fig. 1.

IV. Validation

The results of velocity profile for flow are presented with help of cylindrical coordinates, where the x – axis of the system is dimensionless axial flow axis and radial direction axis along the gap of annular pipe of four sectors (A, B, C, and D) as shown in Fig. (1). The calculated results for ε = 0.2, 0.5 for rotation of inner cylinder Re = 115 and Ta = 3000 are in good agreement with the velocity profile data of reference [4]. The mass flow rate used to determine the axial velocity value.

Figs. (3 to 8) were represented profile of axial and tangential velocity components with dimensionless are plotted as a function of the dimensionless position gave agreement between the results of FLUENT (6.2) and reference [4] of the sectors (A, B, C, and D) at ε = 0.2 also the sectors (A and C) at ε = 0.5.

V. Results

Numerical results are achieved by FLUENT (6.2) to solve continuity and momentum (Navier-Stokes equations) in 3D-steady state, cylindrical coordinates. The results are presented in Figs. (9, 10, 11, and 12) which is represented the relationship between non-dimensional distance from wall of inner cylinder toward radial to outer diameter (ξ) and non-dimensional axial velocity (u) of four sectors (A, B, C, and D) varying with the value of angular speed of inner cylinder for ranges (0, 50, 100, 150, 200, and 250) rpm at ε = 0.2. While Figs. (14, 15, 16, and 17) similarly to the pervious figures except eccentricity is equal to 0.4. Figs. (13 & 18) are represented pressure drop or gradient (Pa/m) with angular speed of inner cylinder (rpm) at ε = 0.2 & 0.4 respectively.

For all cases at ω > 0 rpm max. axial velocity will be not at center due to rotation affect on profile of axial component. Therefore add drift on center location. Figs. (9 to 12) for that have eccentricity of 0.2 shows effect increases of angular speed of inner cylinder on axial velocity in relative to sector (A), note that axial velocity is decrease with the increasing in rotation speed gradually, while sector (C) this velocity increases when rotation speed is increasing, but sector (B) no rotation inner cylinder the values of axial velocity will be smaller than in case rotation after ω increase from 100 to 250 rpm lead to values of axial velocity is decrease above non-rotation values. But for sector (D) the values of axial velocity will decreases when inner cylinder is rotate also after ω increase from 50 to 250 rpm will lead to axial velocity values increases along the annular gap.

Figs. (14 to 17) represents will the effect of inner cylinder rotation on profile of axial velocity along radial direction of annular passage in four region sectors (A, B, C, and D) that have eccentricity of 0.4, for all cases each curve at ω = 0 is symmetrical and max. Value at ξ = 0.5 but when start

inner cylinder with rotation, the profile of axial velocity will draft away from $\xi = 0.5$ due to the rotation will generate a component will added to the axial velocity. This effect is very small at sector (C). When rotation began increasing of inner cylinder in sectors B & C axial velocity increases with increasing the angular speed of inner cylinder.

While sector (A) related inversely between u and ω. Finally sector (D) have a different behavior compared with the other cases where $\omega = (150 – 250)$ rpm with increasing of axial velocity.

Finally Figs. (13 & 18) shows increasing the pressure drop with angular speed increase in both cases i.e., $\varepsilon = 0.2$ & 0.4, note increasing in pressure drop at $\varepsilon = 0.2$ greater than it's at $\varepsilon = 0.4$.

The nature of the increase in the axial pressure gradient is clearly a function of the geometry of the annulus.

The effect of inertia on the axial pressure gradient, briefly, the effect of inertia is to increase the magnitude of the axial pressure gradient, and the size of this increase is a function of inner-cylinder rotation speed and the geometry of the annulus in question. Ultimately, these inertial effects must arise from the coupling of the equations in the Navier–Stokes set as the flow is three-dimensional [9].

Thus two graphs are shown that increasing of angular speed of inner cylinder lead to increase in pressure drop on two extreme edge of pipe.

VI. CONCLUSIONS

1. The results gave good agreement with other published researchers.
2. Axial velocity at sector (A) increase with increasing of angular speed of inner cylinder at $\varepsilon = 0.2$ and 0.4.
3. Axial velocity decrease with increasing of angular speed of inner cylinder in sector (C) at $\varepsilon = 0.2$, also in sectors (B, C) at $\varepsilon = 0.4$.
4. When inner cylinder start to rotate axial velocity profile become non-symmetrical about centerline radial gap of passage.
5. Pressure gradient increase with increasing of angular speed in both case i.e., $\varepsilon = 0.2$, 0.4 but at $\varepsilon = 0.2$ greater than at $\varepsilon = 0.4$ along range of angular speed i.e., $\omega = (0$ to 250) rpm.

REFERENCES

[1] C. Shu, L. Wang, Y. T. Chew, N. Zhao, "Numerical Study of Eccentric Couette – Taylor Flows and Effect of Eccentricity on Flow Patterns", Theoretical Computational Fluid Dynamics, Vol. 18, pp. 43 – 59, 2004.

[2] Hua-Shu Dou, Boo Cheong Khoo, Khoon Seng Yeo, "Energy loss distribution in the plane Couette flow and the Taylor–Couette flow between concentric rotating cylinders", International Journal of Thermal Sciences Vol. 46, pp. 262–275, 2007.

[3] C. H. Ataíde, F. A. R. Pereira e M. A. S. Barrozo, "CFD Predictions Of Drilling Fluids Velocity Profiles In Horizontal Annular Flow", 2nd Mercosur Congress on Chemical Engineering, 4th Mercosur Congress on Process Systems Engineering, ENPROMER, Costa Veroe-Rj-Brazil, 2003.

[4] Escudier, M.P., Gouldson, I.W., Oliveira, P.J., Pinho, F.T., "Effects of inner cylinder rotation on laminar flow of a Newtonian fluid through an eccentric annulus", Int. J. Heat Fluid Flow, Vol. 21, p. 92–103, 2000.

[5] Escudier, M. P.; Oliveira, P. J.; Pinho, F. T.; Simth, S., "Fully developed laminar flow of purely viscous non-Newtonian liquids annuli, Including the effects of eccentricity and inner – cylinder rotation", International Journal of Heat and Fluid Flow, Vol. 33, p. 52-73, 2002.

[6] M. Carrasco Teja & I. A. Frigaard, "Displacement flows in horizontal, narrow, eccentric annuli with a moving inner cylinder", Physic of Fluids, Vol. 21, 073102, 2009.

[7] J.M. Nouri, H. Umur; J.H. Whitelaw, "Flow of Newtonian and non-Newtonian fluids in concentric and eccentric annuli", *J. Fluid Mech.*, Vol. 253, pp. 617-641, 1993.

[8] Md Mamunur Rashid**,** "CFD for Newtonian Glucose fluid flow through concentric annuli with centre body rotation", International Journal on Science and Technology (IJSAT) Vol. II, Issue V, pp. 180 – 186, 2008.

[9] S.Wan, D. Morrison, and I.G. Bryden, "The Flow of Newtonian And Inelastic Non-Newtonian Fluids in Eccentric Annuli With Inner-Cylinder Rotation", Theoret. Comput. Fluid Dynamics, Vol. 13, pp. 349–359, 2000.

RECOMMENDATIONS

An extension of the present work is recommended for a future works includes:

1. Investigation of the unsteady flow and study the vortex shedding process.
2. Study effect of rotation of outer cylinder as well as rotation of inner cylinder.
3. Study effect of entrance length that happened before fully developed flow region.
4. Insert effect of gravity of fluid on the pressure and velocity profile.
5. Take in consider the inner cylinder rotates at high rotational speed (turbulence model).

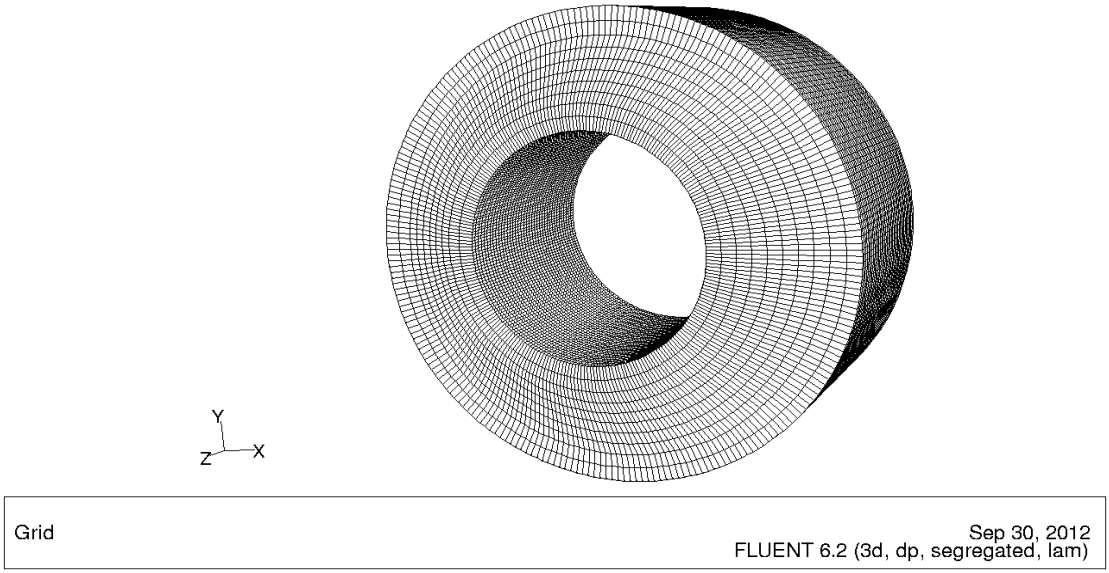

Fig. 1. Grid generation of ε = 0.2, κ = 0.5

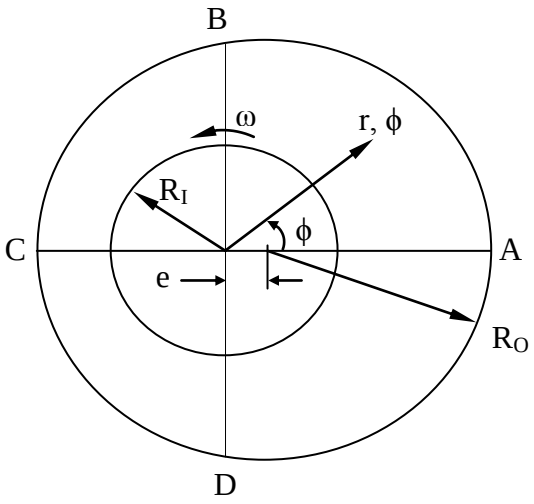

Fig. 2. Annular section in two dimensions with cylindrical coordinate

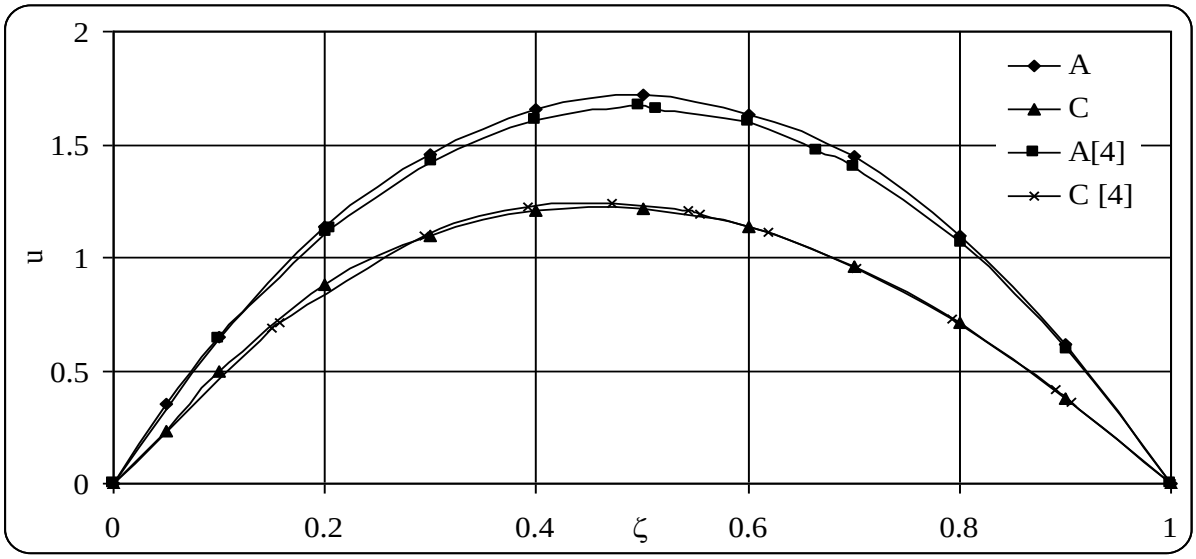

Fig. 3. Comparison between present study and Ref. [4] of non-dimensional axial velocity profile for Re = 105, ε = 0.2 at sectors A and C

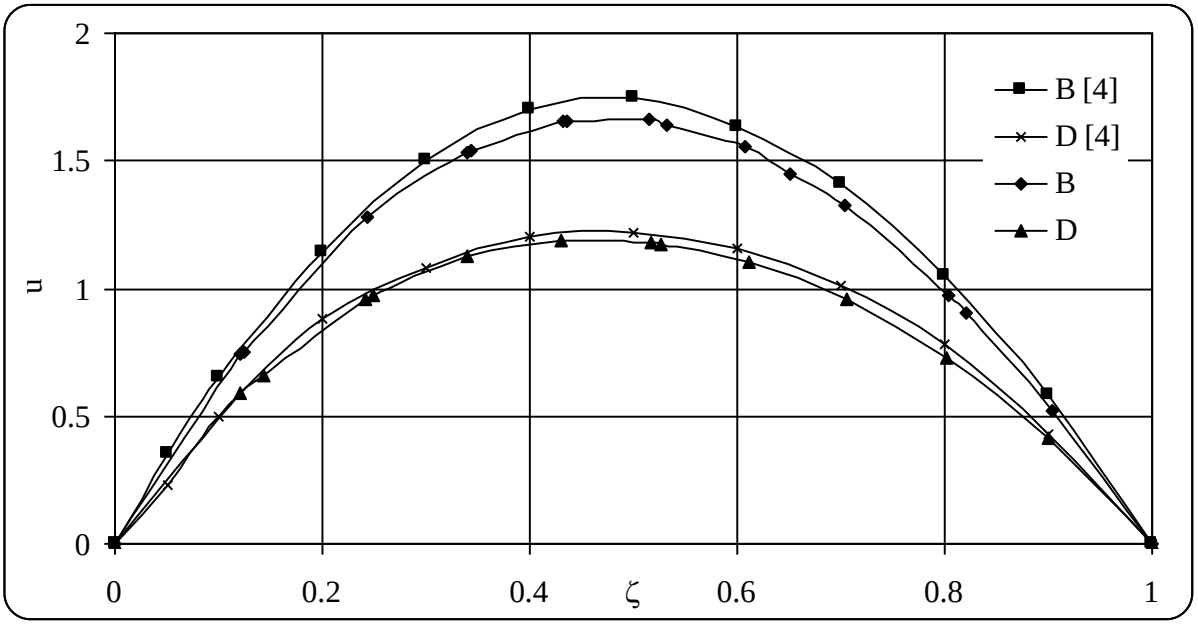

Fig. 4. Comparison between present study and Ref. [4] of non-dimensional axial velocity profile for Re = 105, ε = 0.2 at sectors B and D

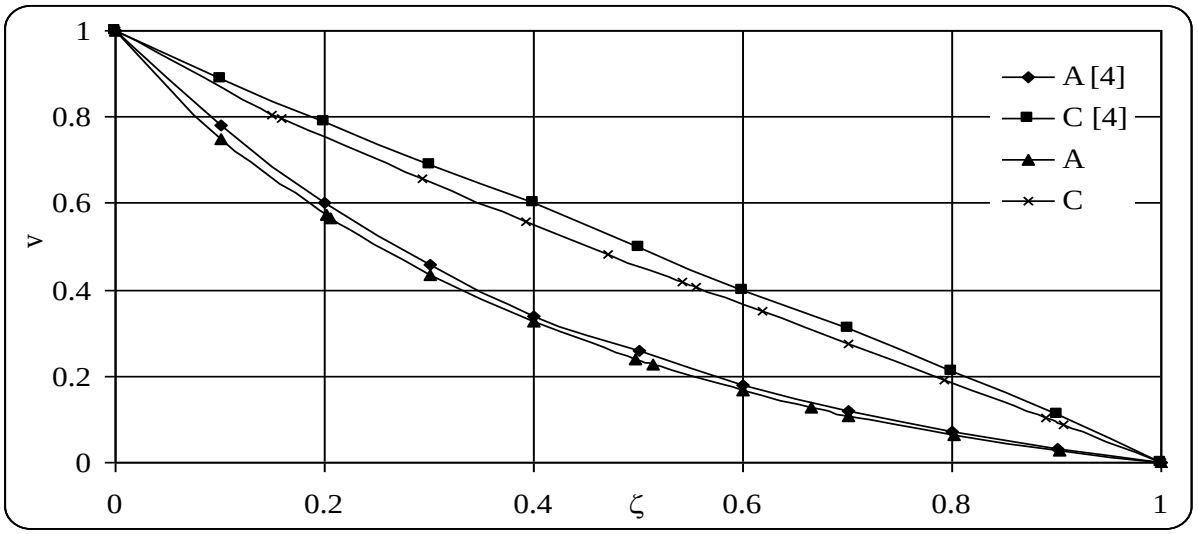

Fig. 5. Comparison between present study and Ref. [4] of non-dimensional tangential velocity profile for Re = 105, ε = 0.2 at sectors A and C

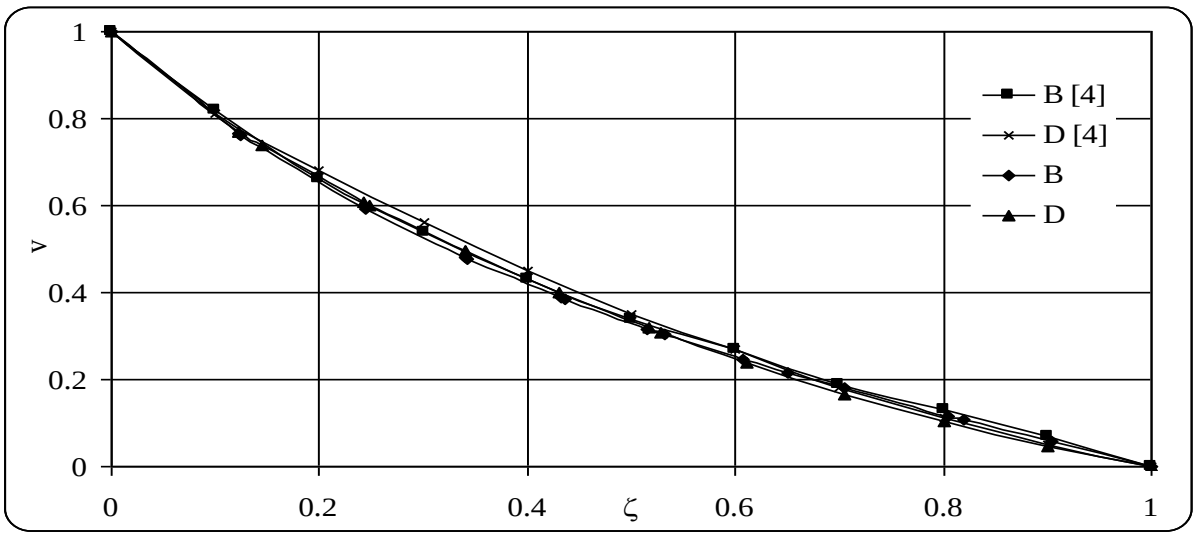

Fig. 6. Comparison between present study and Ref. [4] of non-dimensional tangential velocity profile for Re = 105, ε = 0.2 at sectors B and D

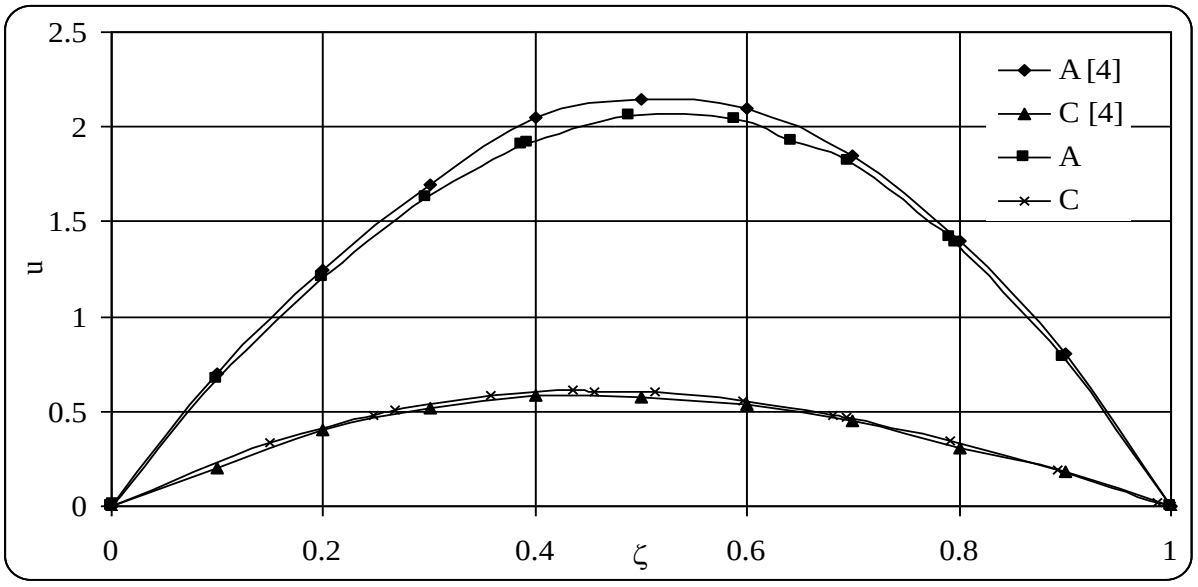

Fig. 7. Comparison between present study and Ref. [4] of non-dimensional axial velocity profile for Re = 105, ε = 0.5 at sectors A and C

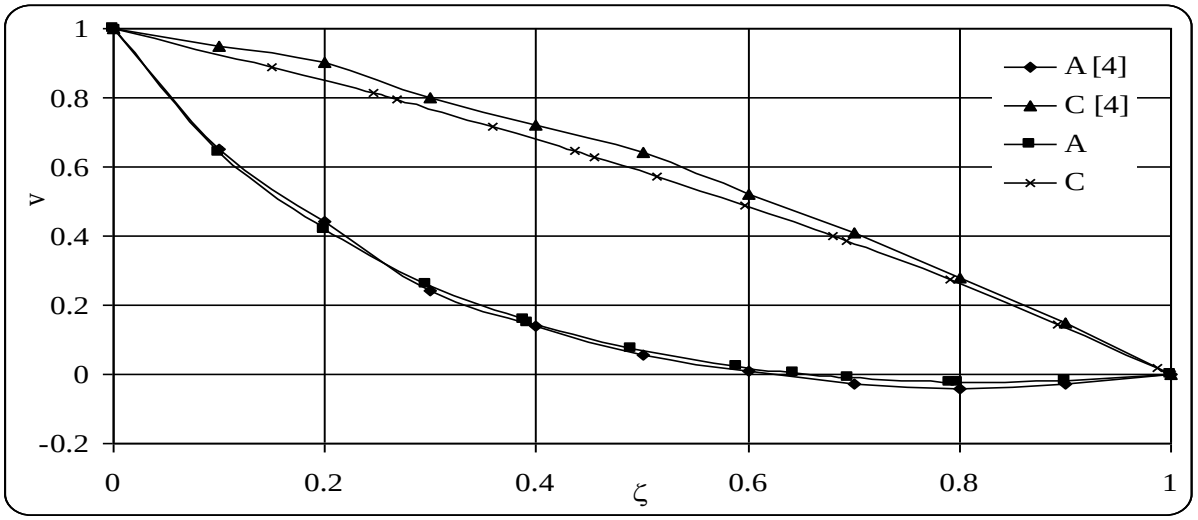

Fig. 8. Comparison between present study and Ref. [4] of non-dimensional tangential velocity profile for Re = 105, ε = 0.5 at sectors A and C

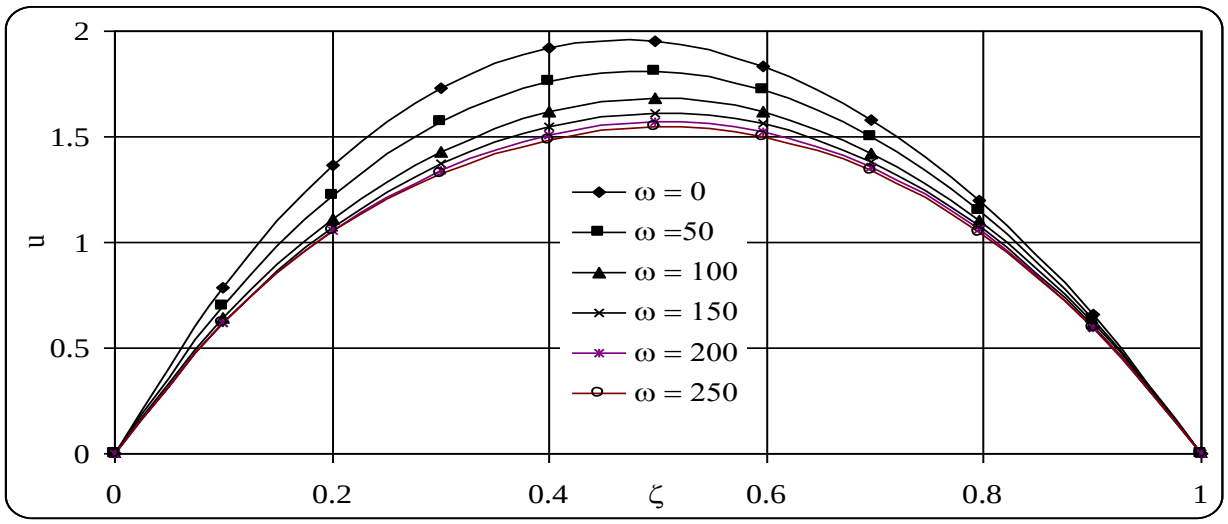

Fig. 9. Non-dimensional axial velocity of sector (A) vs. non-dimensional distance from wall of inner to outer cylinder (radial gap) at ε = 0.2 and κ = 0.5

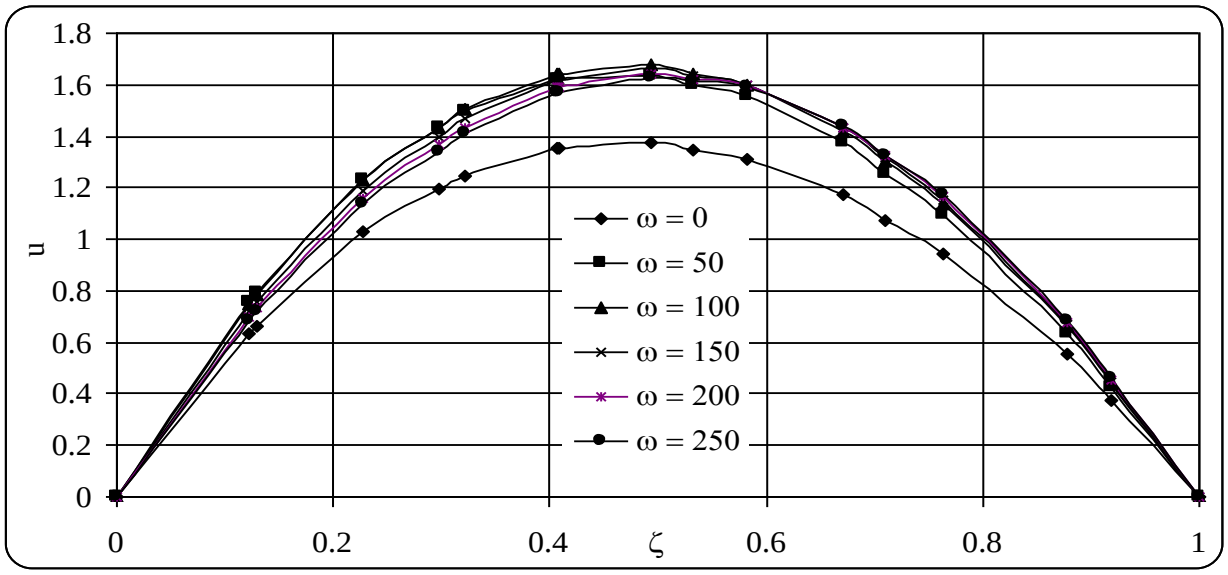

Fig. 10. Non-dimensional axial velocity of sector (B) vs. non-dimensional distance from wall of inner to outer cylinder (radial gap) at ε = 0.2 and κ = 0.5

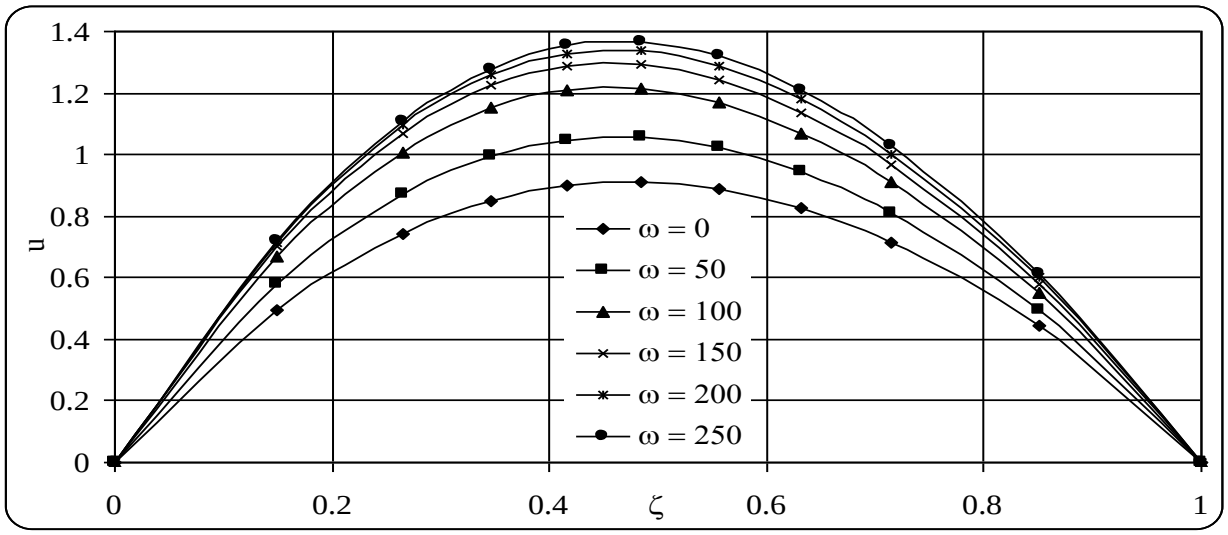

Fig. 11. Non-dimensional axial velocity of sector (C) vs. non-dimensional distance from wall of inner to outer cylinder (radial gap) at ε = 0.2 and κ = 0.5

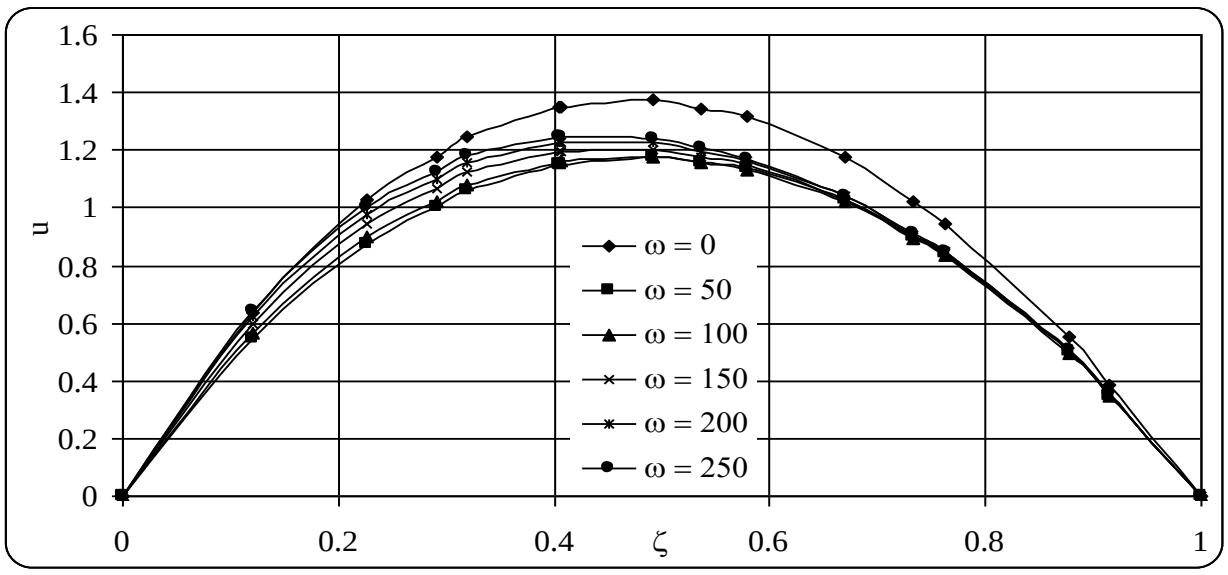

Fig. 12. Non-dimensional axial velocity of sector (D) vs. non-dimensional distance from wall of inner to outer cylinder (radial gap) at ε = 0.2 and κ = 0.5

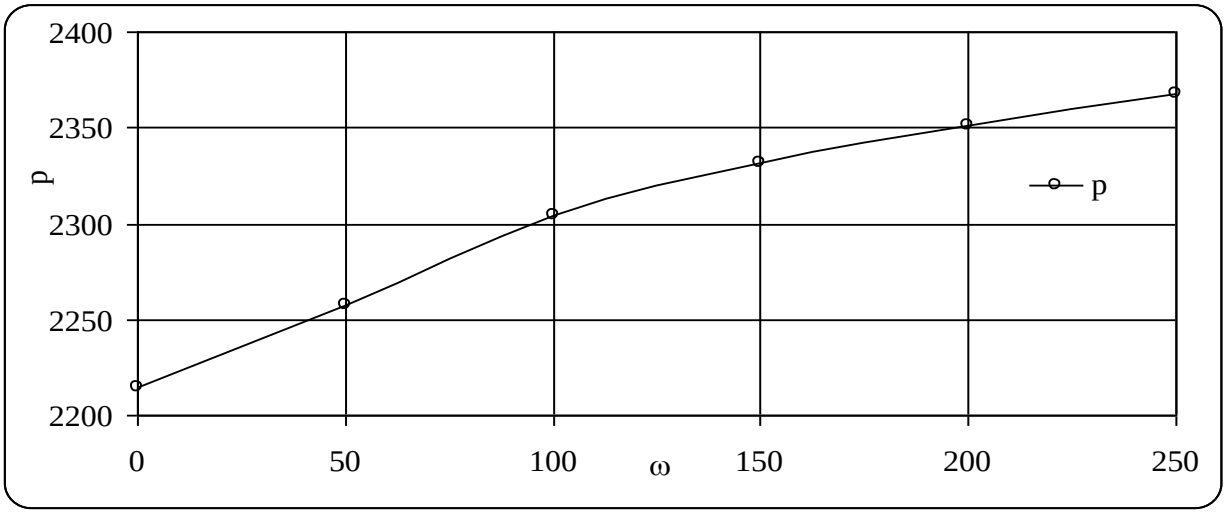

Fig. 13. Axial pressure gradient (Pa/m) vs. inner cylinder rotation (rpm) at ε = 0.2, κ = 0.5

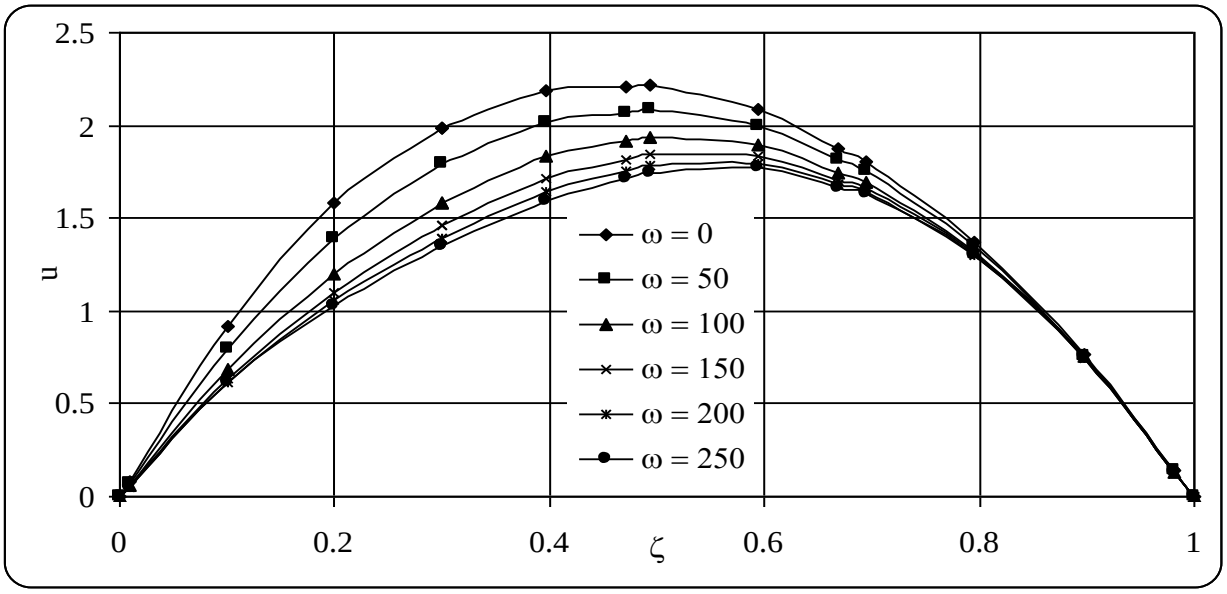

Fig. 14. Non-dimensional axial velocity of sector (A) vs. non-dimensional distance from wall of inner to outer cylinder (radial gap) at ε = 0.4 and κ = 0.5

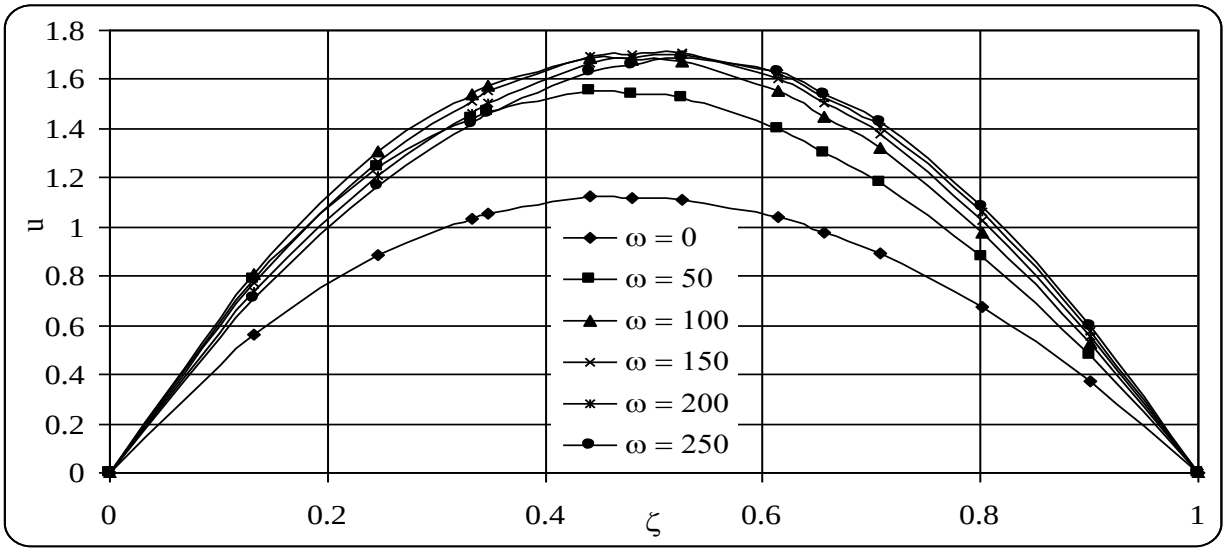

Fig. 15. Non-dimensional axial velocity of sector (B) vs. non-dimensional distance from wall of inner to outer cylinder (radial gap) at ε = 0.4 and κ = 0.5

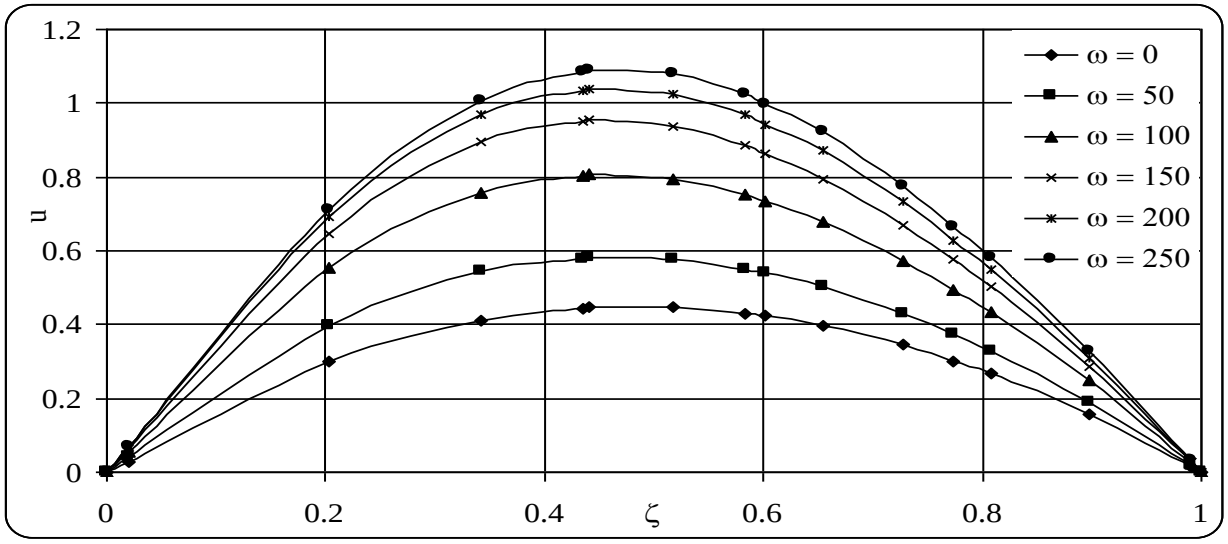

Fig. 16. Non-dimensional axial velocity of sector (C) vs. non-dimensional distance from wall of inner to outer cylinder (radial gap) at ε = 0.4 and κ = 0.5

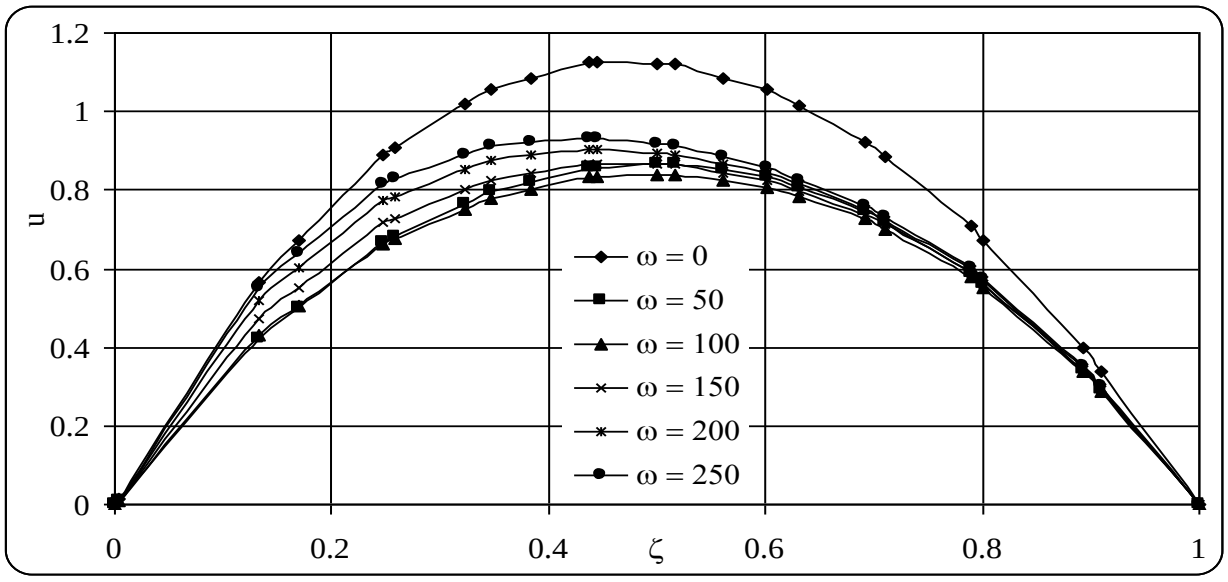

Fig. 17. Non-dimensional axial velocity of sector (D) vs. non-dimensional distance from wall of inner to outer cylinder (radial gap) at ε = 0.4 and κ = 0.5

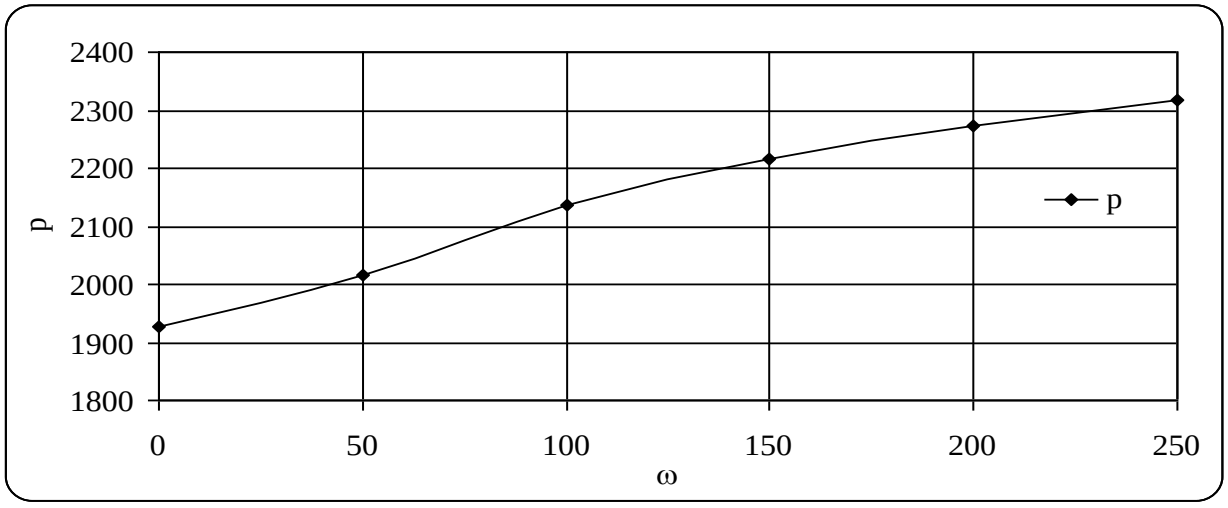

Fig. 18. Axial pressure gradient (Pa/m) vs. inner cylinder rotation (rpm) at ε = 0.4, κ = 0.